ELSEVIER

Journal of Contaminant Hydrology 21 (1996) 87–100

JOURNAL OF
Contaminant
Hydrology

The Grimsel (Switzerland) migration experiment: integrating field experiments, laboratory investigations and modelling

Jörg Hadermann *, Walter Heer

Paul Scherrer Institute, CH-5232 Villigen PSI, Switzerland

Received 17 December 1993; accepted 15 December 1994 after revision

Abstract

For several years tracer migration experiments are performed at Nagra's Grimsel Test Site in the Swiss Alps as a joint undertaking of Nagra, PNC and PSI. The aim is to develop methods for field experiments at possible sites for nuclear waste repositories and to test radionuclide transport models.

A hydraulic dipole field is generated in a well-defined fracture zone in granite. The tracers used are non-sorbing (uranine, ^{3}He, ^{4}He, $^{82}Br^{-}$, $^{123}I^{-}$), mildly sorbing ($^{22}Na^{+}$, $^{24}Na^{+}$), and more strongly sorbing ($^{85}Sr^{2+}$, $^{86}Rb^{+}$, $^{134}Cs^{+}$, $^{137}Cs^{+}$). These experiments have been complemented by extensive laboratory investigations on petrography, on water–rock and nuclide–rock interaction as well as by migration experiments with bore cores.

The main questions addressed are: What are the relevant geometric factors and mechanisms for transport, how well can breakthrough curves be extrapolated from one dipole arrangement to another, which parameters are scale dependent, is there a difference in sorption values between laboratory and field experiments or between static and dynamic experiments. Evaluating the experimental results for the non-sorbing uranine and the mildly sorbing tracers Sodium and Strontium, we show that a consistent picture of tracer transport, and specifically of tracer sorption, is obtained when exploiting all available experimental information and using not too simplistic models.

* Corresponding author.

SSDI 0169-7722(95)00035-6

1. Introduction

In Switzerland, disposal of high-level and long-living intermediate-level radioactive wastes is planned in deep-lying crystalline rock. The safety of such a repository relies, among other factors, on the barrier function of the host rock. Therefore, models of radionuclide transport are important components of safety assessment. In Switzerland, as elsewhere (e.g., NEA/SKI, 1992), testing of such models is a crucial and long-lasting activity.

To this end, and in order to develop methods for site characterisation, Nagra (Swiss National Cooperative for the Disposal of Radioactive Waste), PNC (Power Reactor and Nuclear Fuel Development Corporation, Japan) and PSI (Paul Scherrer Institute, Switzerland) are performing an integrated migration experiment at Nagra's Grimsel Test Site (GTS) since 1985. In this, extensive fieldwork is complemented by a substantial programme of hydrodynamic, chemical and transport modelling, along with supporting laboratory studies (Frick et al., 1992). At GTS, the location for the migration experiment has been selected such as to minimise uncertainties from the geometrical structure of the medium. A steady-state dipole water flow field is generated in a well-defined fractured shear-zone of the crystalline rock. The effect of the natural flow field can be neglected. Investigating tracer breakthrough in such a dipole field yields parameters averaged in a natural way.

The aims of modelling field tracer transport and of the parallel integration of results from laboratory experiments is three-fold: (1) to achieve an improved understanding of nuclide transport; (2) to gain information on validity of methods and data; and (3) to improve modelling for safety assessments.

The paper is organised as follows: In the following two sections we give a very short summary of the main features of the experiment and on the conceptual model underlying the tracer transport evaluation, respectively. For more details the reader is referred to Heer and Hadermann (1994). In the next section the model is applied to the analysis of selected tracer migration experiments. These include experiments with the non-sorbing tracer uranine, the mildly sorbing tracer ^{22}Na and the more strongly sorbing tracer ^{85}Sr. The methodology is to calibrate tracer-independent data with conservative tracer data and then, keeping those parameters fixed, to investigate transport of sorbing tracers. Here, also a comparison to sorption data from other than the migration field experiments is done. Predictions are next made for a new dipole arrangement and compared to subsequent experiments. Finally, conclusions are shortly summarised in the last section.

2. Main experimental features

To provide the experimental information necessary to understand the basic ideas of the model, the main features of the migration experiments at GTS are briefly summarised. A detailed description of the site and the experimental set-up is given in Frick et al. (1992) and specific experimental details and testing results are presented in Eikenberg et al. (1994).

Two bore-holes are drilled from the GTS tunnel into the fractured shear-zone. The intersection of the bore-holes and the fracture is packed off. In one bore-hole water is

injected, and extracted from the other at a higher rate. By choosing appropriate water injection and extraction rates, a dipole field is generated such that full tracer recovery at the extraction hole can be expected. Typical data are: injection rate $Q_i = 9$ mL min^{-1}, extraction rate $Q_w = 150$ mL min^{-1}, distance between injection and extraction point $L_0 = 2–5$ m. To investigate nuclide transport, a pulse of tracer nuclides with different properties is added to the injected water. Tracer pulse advection and dispersion in the injection tubing is taken into account by measuring the tracer distribution down-hole at the injection point of the fracture (optical quartz fiber fluorometry). Natural Grimsel water pumped from the same fracture, but from a location outside the dipole region, and closed under cover gas atmosphere is used for injection, so that the tracer behaviour within the fracture is not influenced by a possibly disturbed water chemistry. The results of the experiments are tracer breakthrough concentrations determined at the extraction point of the fracture (fluorometry for uranine and γ-detection with a Na scintillator for ^{22}Na and ^{85}Sr).

3. Models

This section gives a short summary of the models used in the interpretation of the migration experiments. They are conveniently split into a hydrological and a transport model, respectively. For a more extensive description the reader is referred to Herzog (1989,1991) and Jakob et al. (1989).

The description of the *hydrology*, relevant for the migration experiment, relies on the following basic *hypotheses*:

(1) The migration zone, defined as that part of the fractured shear-zone which is important for the migration experiment, can be represented by a confined planar aquifer. The validity of this assumption is corroborated by geological investigations (Bossart and Mazurek, 1991).

(2) The flow in the aquifer obeys Darcy's law (equation of viscous fluid motion averaged over a representative elementary volume and neglecting drag forces and compressibility).

(3) The migration zone can be characterised by an average homogeneous isotropic transmissivity, T, and by an average homogeneous flow porosity, ϵ. The first assumption is based on an evaluation of interference tests and hydraulic modelling (Herzog, 1989).

(4) The flow field is an unperturbed dipole field governed completely by position and pumping rate of the injection and the extraction well. This is a reasonable approximation since the migration zone is positioned in a region where the hydraulic potential field is flat for closed wells.

(5) The dipole flow field is stationary for one single experiment. This has been repeatedly tested by injecting non-sorbing tracers and measuring breakthrough.

With these assumptions a dipole flow field can be calculated (Fig. 1) for the fracture zone. The dipole field can be divided into two parts: An inner region, defined by all flow lines originating at the injection hole. If the extraction pumping rate is larger than the injection rate, these flow lines end in the extraction hole; and, secondly, an outer

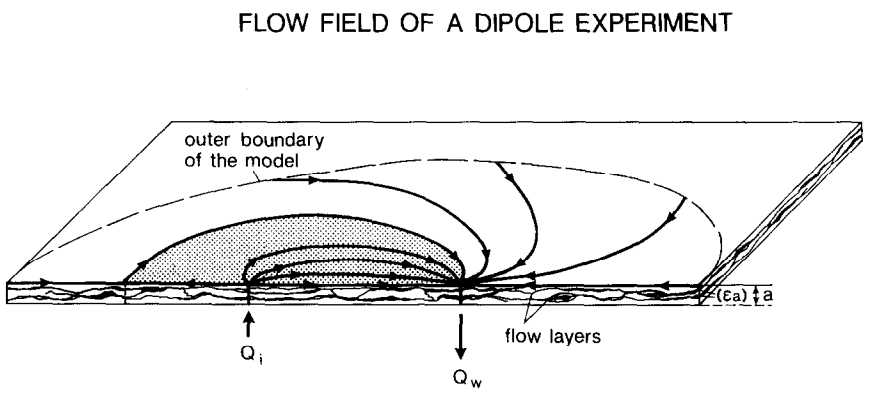

Fig. 1. Dipole flow field in the fractured shear-zone of thickness a and flow porosity ϵ. Q_i and Q_w indicate injection and withdrawal locations/rates, respectively. A few *stream lines* are drawn and the *shaded area* represents the region of stream lines running from Q_i to Q_w.

region then contributing to dilution in the withdrawal hole. The inner flow field is divided into k_{max} stream tubes, typically ten. For each stream tube an average velocity, $\bar{v}_k$ and a migration distance L_k can be calculated.

The tracer breakthrough concentration, $C_f(t)$, in the extraction hole is then given by the superposition of contributions of individual stream tubes, $C_{fk}(t)$:

$$C_f(t) = \left(\frac{Q_i}{Q_w}\right) \frac{1}{k_{max}} \sum_{k-1}^{k_{max}} C_{fk}(t) \tag{1}$$

Here, $C_{fk}(t)$ is the solution of the transport equations (2) and (6). Transversal dispersion from one stream tube to the adjacent ones is neglected since transversal dispersivity and gradient are small. The ratio $Q_i/Q_w \leq 1$ is a dilution factor.

Investigations on structural geology (Bossart and Mazurek, 1991) show that water flow is taking place mainly in a small number of interconnected fractures which are partially filled with highly porous micaceous fault gouge. They are embedded in a fabric of granitic rock exhibiting an enlarged pore space. Connected porosity containing stagnant water as well as additional interconnections of the main fractures and small flow paths parallel to the main flow direction characterise this rock zone.

Correspondingly, the *tracer transport model* is based on the dual porosity concept (Fig. 2) and the following assumptions are made:

(1) Nuclide concentrations as well as transport parameters are macroscopic continuum quantities.

(2) Time and space dependence of macroscopic transport parameters are neglected.

(3) Dispersion in the water-conducting zones accounts for microscopic interconnections between and spacial variability of the zones. In the continuum, it is described by Fick's law. In addition, one has to note that Fick's law represents reality only a few dispersion lengths away from boundaries or discontinuities.

(4) Longitudinal molecular diffusion in the water-conducting zone is neglected with respect to dispersion.

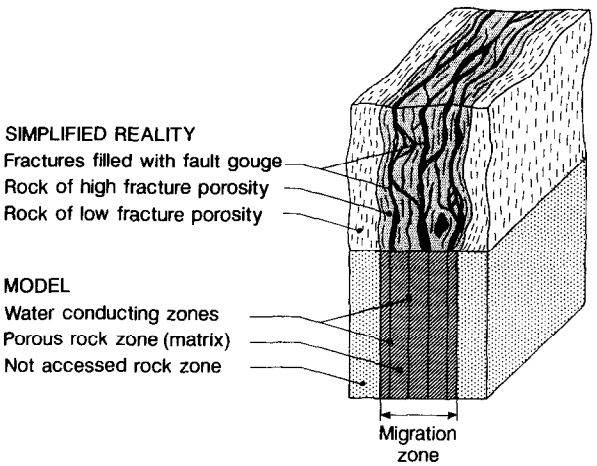

Fig. 2. Based on information on structural geology from bore cores (upper part of figure) a model concept for the geometrical structure important in tracer transport is derived (lower part of figure).

(5) The porous rock zone in the model is a mixture of fault gouge and the adjacent rock. It is characterised by a single set of average parameters.

(6) Matrix diffusion in the water of the porous rock zone is modelled perpendicular to the flow direction.

(7) Sorption on the surfaces of the water-conducting zones as well as on the pore surfaces of the porous rock zone is calculated under the assumption of instantaneous equilibrium. In addition, the sorption isotherm is linear for the tracers considered here.

(8) Individual sorption parameters can be used for the water-conducting and the porous rock zone.

Denoting, now, the coordinate along the stream tube by z, the coordinate into the porous matrix by x, omitting the stream tube index k, and using decay corrected experimental breakthrough curves, the mass balance can be written in the water-conducting zones:

$$\frac{\partial C_f(z,t)}{\partial t} = \frac{1}{R_f}\left[-\bar{v}\frac{\partial C_f(z,t)}{\partial z} + a_L \bar{v}\frac{\partial^2 C_f(z,t)}{\partial z^2} + \frac{\epsilon_p}{b} D_p \frac{\partial C_p(x,z,t)}{\partial x}\bigg|_{x=b} \right] \quad (2)$$

with the boundary conditions

$$\alpha_1 C_f(z=0,t) + \beta_1 \frac{\partial C_f(z,t)}{\partial z}\bigg|_{z=0} = \gamma_1 C_0(t) \quad (3)$$

$$\alpha_2 C_f(z=L,t) + \beta_2 \frac{\partial C_f(z,t)}{\partial z}\bigg|_{z=L} = \gamma_2 \quad (4)$$

At the inlet we have $\alpha_1 = 1$, $\beta_1 = -a_L$, $\gamma_1 = 1$, and at the outlet $\alpha_2 = 0$, $\beta_2 = -1$, $\gamma_2 = 0$. The initial condition is:

$$C_f(z,t=0) = 0 \quad (5)$$

The mass balance for the porous rock zone is:

$$\frac{\partial C_p(x,z,t)}{\partial t} = \frac{1}{R_p} D_p \frac{\partial^2 C_p(x,z,t)}{\partial x^2} \tag{6}$$

The boundary conditions are:

$$C_p(x=b,z,t) = C_f(z,t), \quad 0 < z < L \tag{7}$$

$$\frac{\partial C_p(x=b+d,z,t)}{\partial x} = 0, \quad 0 < z < L \tag{8}$$

and the initial condition is

$$C_p(x,z,t=0) = 0, \quad 0 \le z \le L \tag{9}$$

The retardation factors are given by:

$$R_f = 1 + \frac{1}{b} K_a \tag{10}$$

$$R_p = 1 + \frac{\tilde{\rho}_p}{\epsilon_p} K_d \tag{11}$$

We use the following notation:

$C_f(z,t)$	concentration of tracer in the flowing water
$C_p(x,z,t)$	concentration of tracer in the matrix pore water
$C_0(t)$	injection concentration of tracer
M_0	total tracer mass injected
K_a	area specific sorption distribution coefficient
K_d	mass specific sorption distribution coefficient
$\bar{v}$	water velocity
a_L	longitudinal dispersivity
b	half-width of water-conducting fracture
a	width of fracture zone
ϵ	flow porosity
n	number of water-conducting fractures
ϵ_p	matrix porosity
d	depth of matrix (up to the symmetry plane)
$\tilde{\rho}_p$	bulk density of matrix
D_p	diffusion constant in rock matrix
L	migration distance.

Eqs. 2 and 6 are solved by the computer code RANCHMD. One of the aims of the present work is to evaluate the effect of matrix diffusion. To this end, it is helpful to consider analytical solutions to the transport equations. If the tracer input is sufficiently short, and dispersion and nuclide concentration in the matrix at $x = b + d$ are all the

time sufficiently small (see, e.g., Jakob and Hadermann, 1994), the tracer maximum at the outlet comes at:

$$t_m \approx \frac{LR_f}{\bar{v}} + \tfrac{2}{3}\tau_0 \tag{12}$$

and the concentration is for $t \gg t_m$

$$C_f(L,t) \approx \frac{M_0}{Q_w}\frac{\sqrt{\tau_0}}{\sqrt{\pi}} t^{-3/2} \tag{13}$$

The time shift τ_0 is given by:

$$\tau_0 = \left(\frac{\epsilon_p}{b}\right)^2 \left(\frac{L}{\bar{v}}\right)^2 \frac{D_p R_p}{4} \tag{14}$$

We will use these equations in our discussion of experimental results.

4. Analysis of experimental breakthrough curves

Various approaches have been applied for testing transport models with experimental data, especially field data, NEA/SKI (1993). The main problem is on two levels. First, the model concepts and, second, parameters are uncertain. Ideally, one would like, first, to calibrate the model and, then, to make predictions with fully independent new experiments. This was only partially possible.

Our procedure is as follows: First, a few parameters are fixed a priori from independent measurements. Second, nuclide independent parameters are fitted with data from a non-sorbing tracer, uranine. Then, keeping these data fixed, nuclide dependent parameters (sorption, diffusion) are fitted with data from sorbing tracers, Sodium and Strontium. Finally, predictions are made for and compared to new dipole experiments.

4.1. Calibration with the conservative tracer uranine

Four parameters can be adjusted to fit the model to the experimental breakthrough curve. We have chosen the parameter combinations ϵa (determining also the mean velocity $\bar{v}$), $\epsilon_p\sqrt{D_p}$, $1/\sqrt{D_p}$ and a_L.

Table 1
Parameters fixed a priori

Experimental lay-out	$L_0 = 4.9$ m
	$Q_i = 9.3$ mL min^{-1}
	$Q_w = 148.8$ mL min^{-1}
Structural geology	$a = (5^{+5}_{-2.5}) \cdot 10^{-2}$ m
	$n = 4^{+2}_{-1}$
	$\tilde{\rho}_p = 2{,}670 \pm 200$ kg m^{-3}

The upper part gives the value of the bore hole distance for the dipole field and the two pumping rates. Parameters from bore core investigations (Bossart and Mazurek, 1991) are provided in the lower part.

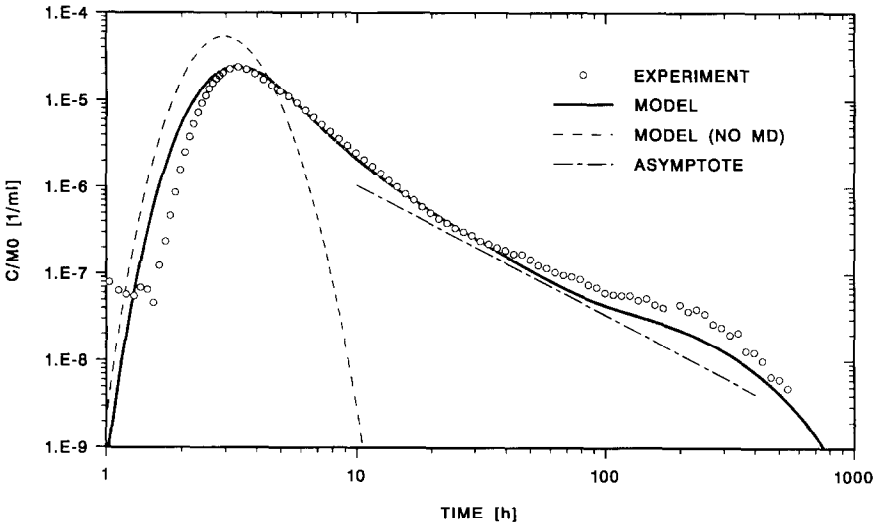

Fig. 3. Experimental breakthrough curve for uranine (*circles*) and model fit (*full line*). Also given is a calculation for a model without matrix diffusion (*short dashes*) and the asymptotic $t^{-3/2}$ decay showing the signature of matrix diffusion, Eq. 13.

Three parameters $(a, n, \tilde{\rho}_p)$ are a priori fixed according to structural geology investigations. Their values with geometric standard deviation are given in Table 1. Further three parameters are defined by the experimental lay-out (L_0, Q_i, Q_w). Here, the errors can be neglected. The input concentration $C_0(t)$ is taken from the down-hole measurement.

The fit of the model to the experimental breakthrough curve for the conservative tracer uranine is depicted in Fig. 3. It is possible to reproduce the full range of the curve rather well. We especially emphasise the agreement of peak value and bump shape in the tail. The corresponding parameters extracted from the fit are given in Table 2. The errors include the contribution of errors in fixed parameters.

The comparison to a calculation without matrix diffusion shows the inadequacy of that model: Within our conceptual model, matrix diffusion is absolutely necessary to represent the experiment. The question arises whether any mechanism other than matrix diffusion could produce such a tail. For times large compared to the peak position, the matrix diffusion mechanism causes a $t^{-3/2}$ dependency resulting from tracer backflow. This is true as long as the outer boundary in the rock matrix is not influencing matrix diffusion. At later times, an increase in the breakthrough concentration arises because of the restriction of further out-diffusion. For still later times, the breakthrough concentration decreases rapidly because of the limited matrix volume. The tail of the experimental breakthrough curve, approaching the asymptote given by the $t^{-3/2}$ slope, and exhibiting the subsequent bump and drop, is a strong support for the dual porosity model.

The extracted parameter values for ϵ_p and D_p are in reasonable agreement with independent measurements (Table 2), especially since the model does not consider the rock matrix heterogeneity. Also the dispersivity is in a range which can be expected from the geometric structure of the water-conducting zones.

Table 2
Parameters extracted from the fit of experimental breakthrough curves (Figs. 3 and 4)

Calibration	$\epsilon a = (3.7 \pm 0.2) \cdot 10^{-4}$ m
Uranine	$\epsilon_p = (6.2^{+6.8}_{-3.2}) \cdot 10^{-2}$
conservative	$a_L = (25^{+5}_{-4}) \cdot 10^{-2}$ m
	$D_p = (2.5^{+11}_{-2.0}) \cdot 10^{-11}$ m^2 s^{-1}
Na	$D_p = (3.3^{+14}_{-2.7}) \cdot 10^{-11}$ m^2 s^{-1}
weakly sorbing	$K_d = (1.3^{+1.6}_{-0.7}) \cdot 10^{-4}$ m^3 kg^{-1}
Sr	$K_d = (2.1^{+3.8}_{-1.4}) \cdot 10^{-2}$ m^3 kg^{-1}
stronger sorbing	
Independent	$\epsilon_p = (1.5^{+1.2}_{-0.7}) \cdot 10^{-1}$
measurements	D_p (uranine) $= (5.5^{+6.1}_{-2.9}) \cdot 10^{-11}$ m^2 s^{-1}
	D_p (Na) $= (1.7^{+1.9}_{-0.9}) \cdot 10^{-10}$ m^2 s^{-1}

The errors are extracted from parameter sensitivity analyses, and are pessimistic guesses for one geometric standard deviation. The independent measurements are evaluated from Bossart and Mazurek (1991) and Frick (1993).

4.2. Sorbing tracers

Besides the question whether the model is also able to reproduce the breakthrough curves, two further issues are of interest. First, do sorption heterogeneities influence the value of dispersivity (Gelhar, 1987), and second, how well do extracted sorption coefficients agree with those of other experiments.

For both, Sodium and Strontium, the parameters R_f and a_L were taken as fit parameters. For Sodium, the two combinations $\epsilon_p\sqrt{D_p R_p}$ and $\sqrt{R_p/D_p}$ were taken as additional fit parameters. For Strontium only one single further combination, $\epsilon_p\sqrt{D_p R_p}$ could be determined since the bump in the tail of the breakthrough curve cannot be seen. A priori fixed was the porosity ϵ_p at its value from uranine, for Strontium a value of $D_p = (2.5^{+2.5}_{-1.3}) \cdot 10^{-11}$ m^2 s^{-1} was taken.

The fits of the model curves are compared to the experimental data in Fig. 4. Especially considering the large differences in time and concentration scale, the agreement is good. Also here, the single porosity model is far off reality. The analytical expression, Eq. 13, is an excellent approximation for the tail (with the exception of the bump for Sodium where the finite extent of matrix is felt). We again see very clearly the effects of matrix diffusion, combined with relatively strong sorption in the case of Strontium.

What concerns the extracted parameter values, we get $R_f = 1$ and $a_L = 0.25$ m, the errors being a few percent. Since no strongly sorbing fracture coatings are detectable and matrix surfaces are much larger than surfaces of water-conducting zones, the first result is comforting. The unchanged value for a_L points to sorption homogeneity in the dipole field. The other parameters extracted are given in Table 2.

We now turn to a comparison of sorption coefficients from various other experiments (Table 3). First are the conventional batch experiments (Aksoyoglu et al., 1990) with

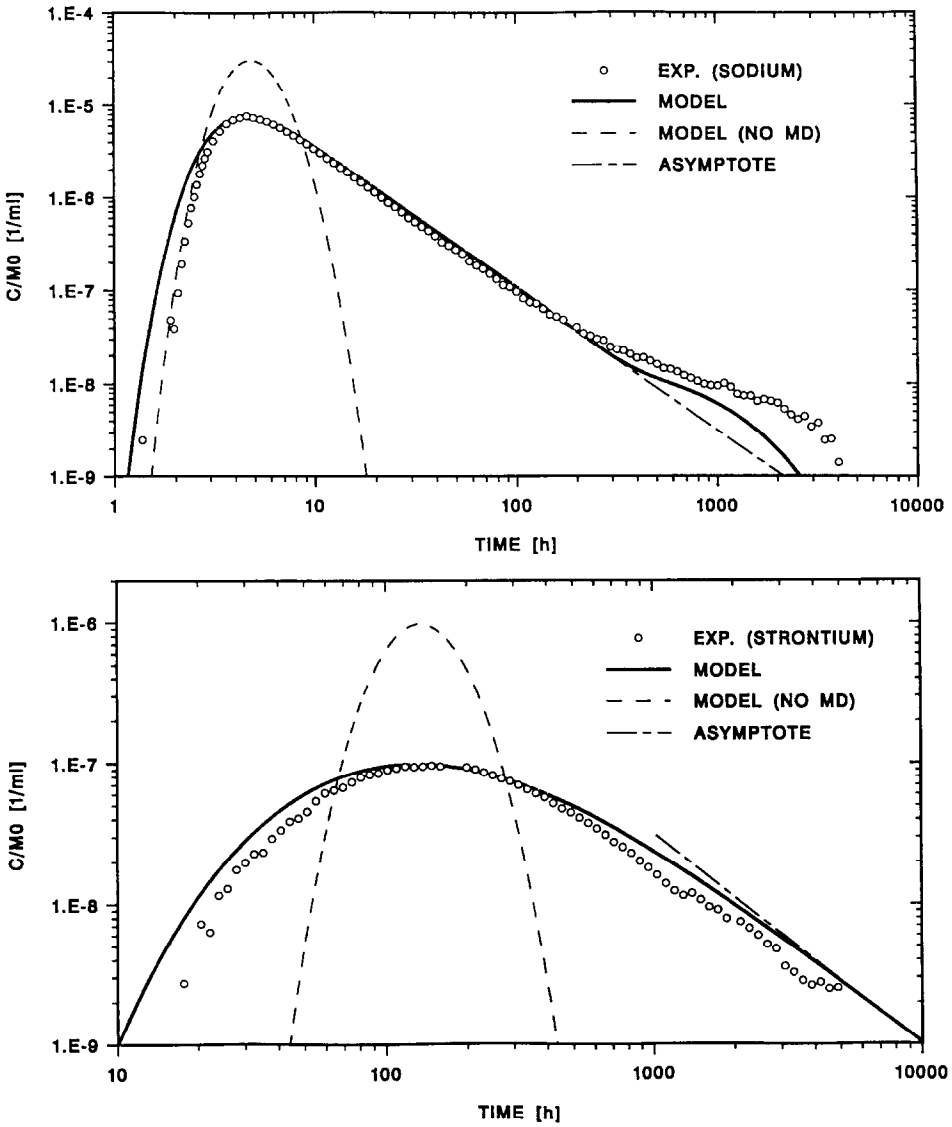

Fig. 4. Experimental breakthrough curves (*circles*) for Sodium (upper part) and Strontium (lower part) compared to the model fit (*full lines*). The *dashed lines* represent a calculation for the single porosity model and the asymptotic analytical solution for the dual porosity model is shown by the *dash–dot lines*.

crushed mylonitic rock from the Grimsel site corrected for the mineral composition in the migration zone. Creation of new surfaces through crushing gives higher values. Rock–water interaction experiments use an ion exchange model for extraction of selectivity coefficients and K_d (Baeyens and Bradbury, 1989). Infiltration experiments are performed on rock cores from the GTS migration zone (water flowpaths in these

Table 3
Comparison of sorption coefficients for Sodium and Strontium from various experiments

	Experiment	K_d (10^{-3} m^3 kg^{-1})	
		Na	Sr
Laboratory	batch (< 63 μm)	$1.3^{+1.5}_{-0.4}$	41^{+39}_{-4}
	batch (< 250 μm)	$0.85^{+0.76}_{-0.04}$	25^{+22}_{-1}
	batch (loosely disaggregated)	$0.43^{+0.60}_{-0.02}$	13^{+19}_{-1}
	rock–water interaction (~ loosely disaggregated)	$0.13^{+0.13}_{-0.02}$	$7.6^{+8.2}_{-1.7}$
	dynamic infiltration	0.1–0.3	
Field	hydrogeochemical	$0.21^{+0.2}_{-0.1}$	7.8^{+8}_{-5}
	migration	$0.13^{+0.16}_{-0.07}$	21^{+38}_{-14}

The experiments include static batch experiments, a rock–water interaction experiment with fracture infill material, and dynamic migration experiments in the laboratory and the field. Except for the first one, sorption coefficients extracted are model dependent.

cores are largely unknown, however) and evaluated much in the same way as the field experiments, but the migration distance is a few centimetres, only (Smith, 1992). The hydrochemical experiment, finally, is a dipole experiment at the GTS using water from a different location and measuring breakthrough of major water constituents (Eikenberg et al., 1991). Here, again an ion exchange model is used to extract sorption coefficients.

Within a factor of three, the different sorption coefficients do agree. This is a gratifying situation and implies that for waste repository assessments, laboratory data can be used without applying excessive reduction factors, provided sorption kinetics is fast compared to migration time scales.

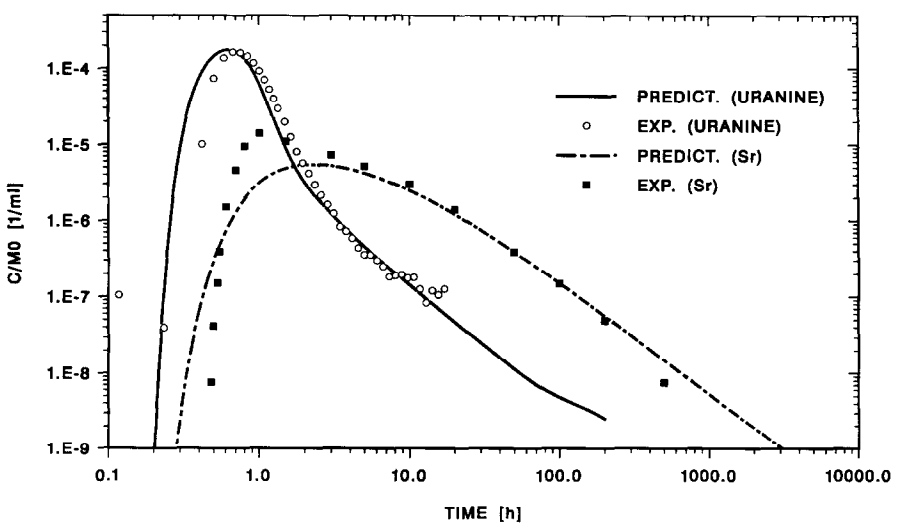

Fig. 5. Comparison of predicted and subsequently measured breakthrough curves of uranine (*full curve, circles*) and Strontium (*dash–dot curve, squares*) for the smaller dipole field.

5. Predictions

Having carried out and evaluated the 4.9-m dipole experiments, predictions were made with the calibrated model prior to the experiment in a 1.7-m dipole field. The comparison is shown in Fig. 5 for uranine and Strontium (Sodium is not too different from uranine). For both tracers, the agreement is rather well. Especially is this the case for Strontium where peak height and time are strongly different compared to the 4.9-m dipole.

Matrix diffusion is much less effective (compare Eq. 14), and the finite extent of rock matrix would show up at concentrations below detection limit. However, Strontium nicely shows the $t^{-3/2}$ dependence in the tail. Based on yet unevaluated Cesium experiments, we feel that an influence of sorption kinetics turns up in the peak region. Hence, the sharper rise and greater height in the experimental data. The model does not include such a mechanism.

In essence, this agreement implies that parameter dependencies are correctly simulated by the model (within the range investigated). Since the two different dipole fields are somewhat orthogonal in the shear-zone plane, it also shows that natural variability is small (within the region investigated).

6. Conclusions

We have investigated and discussed uranine, Sodium and Strontium tracer migration experiments at the Grimsel Test Site. Model parameters were extracted from best-fit breakthrough curves and compared to data from independent measurements. Keeping these parameters fixed, predictions for breakthrough were made and compared to subsequent field experiments. The following conclusions can be drawn:

(1) No new process had to be invoked in order to model the breakthrough curves or to justify particular parameter values. The model is able to describe the breakthrough curves of the migration field experiments to a large degree of accuracy. Having a few number of free parameters, this is a strong indication that it contains the relevant mechanisms governing tracer transport.

(2) Diffusion into zones of stagnant water is absolutely necessary to model the Grimsel experiments. Tracer is transported advectively and dispersively in narrow water-conducting zones.

(3) Matrix diffusion not limited by a boundary condition is manifest through the tail of the breakthrough curve decreasing with $t^{-3/2}$.

(4) Only if the breakthrough curve is measured down to the tail end over many orders of magnitude, indicating matrix diffusion up to the symmetry plane, a separate determination of D_p and ϵ_p is possible for a conservative tracer, and of D_p and R_p for a sorbing tracer.

(5) Experiments with sorbing tracers show a negligible surface sorption ($R_f = 1$) and a tracer-independent dispersion length a_L.

(6) The sorption constants for Sodium and Strontium, determined in the migration field experiments, are encouragingly consistent with the corresponding values deter-

mined in other experiments. This shows that sorption constants from laboratory experiments can be used for the field if adequate care is taken in sample selection and preparation.

(7) The model was able to predict reasonably well the influence of a change in flow field from a 4.9-m dipole to a 1.7-m dipole. The prediction of the conservative tracer uranine and Sodium is excellent, that of the sorbing Strontium adequate, indicating possibly sorption kinetics.

The Grimsel migration experiment is a very useful test of model and data. The results of the analysis are an important step in building confidence in the calculational methods and data.

During preparation of this paper a series of further field experiment has been performed, notably with the strongly non-linearly sorbing tracer Cesium. Modelling of these experiments is the subject of a forthcoming paper (W. Heer et al., in prep.).

Acknowledgements

We would like to thank Th. Fierz, U. Frick, E. Hoehn, M. Mazurek and J. Eikenberg for their continual communication of the newest field results and for discussions. The comparison to laboratory data has greatly profited from discussions with B. Baeyens and M. Bradbury. Also discussions on modelling aspects with A. Jakob, P. Smith and C.-F. Tsang are gratefully acknowledged, as well as general discussions with I. McKinley and within the INTRAVAL community. Finally, we thank Nagra for partial financial support.

References

Aksoyoglu, S., Bajo, C. and Mantovani, M., 1990. Batch sorption experiments with iodide, bromine, strontium, sodium and cesium on Grimsel mylonite. PSI (Paul Scherrer Inst.), Würenlingen, PSI-Ber. No. 83 and Nagra (Natl. Coop. Disposal Radioactive Waste), Wettingen, Nagra NTB 91-06.

Baeyens, B. and Bradbury, M., 1989. Selectivity coefficients and estimates of in-situ sorption values for mylonite. In: M. Bradbury (Editor), Laboratory Investigations in Support of the Migration Experiments at the Grimsel Test Site. PSI (Paul Scherrer Inst.), Würenlingen, PSI-Ber. No. 28 and Nagra (Natl. Coop. Disposal Radioactive Waste), Wettingen, Nagra NTB 88-23.

Bossart, P. and Mazurek, M., 1991. Grimsel Test Site: Structural geology and water flow-paths in the migration shear-zone. Nagra (Natl. Coop. Disposal Radioactive Waste), Wettingen, Nagra NTB 91-12.

Eikenberg, J., Baeyens, B. and Bradbury, M., 1991. The Grimsel migration experiment: A hydrogeochemical equilibrium test. PSI (Paul Scherrer Inst.), Würenlingen, PSI-Ber. No. 100 and Nagra (Natl. Coop. Disposal Radioactive Waste), Wettingen, Nagra NTB 90-39.

Eikenberg, J., Hoehn, E., Fierz, Th. and Frick, U., 1994. Grimsel Test Site: Preparation and performance of migration experiments with radioisotopes of sodium, strontium and iodide. PSI (Paul Scherrer Inst.), Würenlingen, PSI-Ber. No. 94-11 and Nagra (Natl. Coop. Disposal Radioactive Waste), Wettingen, Nagra NTB 94-17.

Frick, U., 1993. Beurteilung der Diffusion im Grundwasser von Kristallingesteinen. Nagra (Natl. Coop. Disposal Radioactive Waste), Wettingen, Intern. Rep. NIB 92-92.

Frick, U., Alexander, W.R., Baeyens, B., Bossart, P., Bradbury, M.H., Bühler, Ch., Eikenberg, J., Fierz, Th., Heer, W., Hoehn, E., McKinley, I.G. and Smith, P.A., 1992. The radionuclide migration experiment

—Overview of investigations 1985–1990. PSI (Paul Scherrer Inst.), Würenlingen, PSI-Ber. No. 120 and Nagra (Natl. Coop. Disposal Radioactive Waste), Wettingen, Nagra NTB 91-04.

Gelhar, L.W., 1987. Applications of stochastic models to solute transport in fractured rocks. SKB (Swed. Nucl. Fuel & Waste Manage. Co.), Stockholm, Tech. Rep. 87-05.

Heer, W. and Hadermann, J., 1994. Grimsel Test Site: Modelling radionuclide migration field experiments. PSI (Paul Scherrer Inst.), Würenlingen, PSI-Ber. No. 94-13 and Nagra (Natl. Coop. Disposal Radioactive Waste), Wettingen, Nagra NTB 94-18.

Herzog, F., 1989. Hydrologic modelling of the migration site in the Grimsel Rock Laboratory —The steady state. PSI (Paul Scherrer Inst.), Würenlingen, PSI-Ber. No. 35 and Nagra (Natl. Coop. Disposal Radioactive Waste), Wettingen, Nagra NTB 89-16.

Herzog, F., 1991. A simple transport model for the Grimsel migration experiment. PSI (Paul Scherrer Inst.), Würenlingen, PSI-Ber. No. 106 and Nagra (Natl. Coop. Disposal Radioactive Waste), Wettingen, Nagra NTB 91-31.

Jakob, A. and Hadermann, J., 1994. INTRAVAL Finnsjön Test —modelling results for some tracer experiments. PSI (Paul Scherrer Inst.), Würenlingen, PSI-Ber. No. 94-12 and Nagra (Natl. Coop. Disposal Radioactive Waste), Wettingen, Nagra NTB 94-21, Appendix 3.

Jakob, A., Hadermann J. and Rösel, F., 1989. Radionuclide chain transport with matrix diffusion and non-linear sorption. PSI (Paul Scherrer Inst.), Würenlingen, PSI-Ber. No. 54 and Nagra (Natl. Coop. Disposal Radioactive Waste), Baden, Nagra NTB 90-13.

NEA/SKI (Nuclear Energy Agency/Swedish Nuclear Inspectorate), 1992. The International INTRAVAL Project: Phase 1, Test Cases. OECD/NEA (Org. Econ. Coop. Dev./Nucl. Energy Agency), Paris, 157 pp.

NEA/SKI (Nuclear Energy Agency/Swedish Nuclear Inspectorate), 1993. The International INTRAVAL Project, Phase 1, Summary Report, OECD/NEA (Org. Econ. Coop. Dev./Nucl. Energy Agency), Paris, 135 pp.

Smith, P., 1992. Modelling of laboratory high-pressure infiltration experiments. PSI (Paul Scherrer Inst.), Würenlingen, PSI-Ber. No. 116 and Nagra (Natl. Coop. Disposal Radioactive Waste), Wettingen, Nagra NTB 91-33.